JOURNAL OF NANO- AND ELECTRONIC PHYSICS
Vol. 16 No 2, 02030(6pp) (2024)
ЖУРНАЛ НАНО- ТА ЕЛЕКТРОННОЇ ФІЗИКИ
Том 16 № 2, 02030(6cc) (2024)

REGULAR ARTICLE

Properties of the Original Electron-Irradiated LEDs Homojunction GaP, GaAsP and Heterojunction InGaN Structures

T.M. Zahorodnia[1], O.V. Melnychenko[2], V.P. Tartachnyk[3], M.E. Chumak[4,*]

[1] Sumy State University, 40007 Sumy, Ukraine
[2] L.V.Pisarzhevskii Institute of Physical Chemistry NAS of Ukraine, 03028 Kyiv, Ukraine
[3] Institute of Nuclear Research NAS of Ukraine, 02000 Kyiv, Ukraine
[4] Drahomanov Ukrainian State University, 02000 Kyiv, Ukraine

(Received 05 February 2024; revised manuscript received 25 April 2024; published online 29 April 2024)

The work contains a detailed review of the results of research published in recent years on homojunction light-emitting diodes (LEDs) grown on the basis of GaP and GaAsP solid solution, as well as InGaN heterojunction structures with quantum wells (QWs).

In order to identify the cause of the instability of the microplasma glow, it is important to analyze the electrical and spectral characteristics of the studied structures. The purpose of the study was to identify the cause that leads to the deviation from the typical dependences of $I(U)$ and $L(I)$ and to identify possible physical factors that underlie the occurrence of anomalies of the LEDs-radiation.

The original part is based on a comparative analysis of experimental data obtained during the study of the electrophysical and spectral characteristics of both types of LEDs.

The results of the study of the influence of radiation defects introduced by electrons with $E = 2$ MeV on the fundamental and operational parameters of the studied diodes are also presented.

The increase in the differential resistance of homotransient GaP and GaAsP LEDs due to a decrease in temperature and irradiation is caused by the capture of current carriers by deep impurity levels, as well as levels of radiation defects. The value of the barrier potential of the diodes at the doses used ($F_{max} = 10^{15}$ cm^{-2} for GaP diodes; $F_{max} = 2.64$ cm^{-2} for GaAsP diodes) is practically unchanged.

In InGaN heterostructure LEDs with QWs ($h\nu$ = 505 nm) the NDC region begins after cooling to $T \leq 130$ K; its occurrence may be related to the effect of resonant tunneling of current carriers.

The short-wavelength parts of the GaP, GaAsP, and InGaN LEDs emission lines agree well with the classical Gaussian distribution; long-wavelength ones are stretched towards long-wavelengths, which is caused by the effect of the tails of the density of states (TDS) in both homo- and heterotransition structures.

Keywords LEDs, GaP, GaAsP, InGaN, Current-voltage characteristics, Spectral characteristics, Exposure

DOI: 10.21272/jnep.16(2).02030 PACS number: 78.20. – e

1. INTRODUCTION

Solid-state sources of injection light GaP, GaAsP LEDs, grown on the basis of homojunctions, thanks to a simple and cheap production technology, small dimensions, high spectral purity and narrowness of the main emission line, starting from the moment of Golonyak's production (1962) of the first LEDs based on GaAsP, widely used in various fields of electronics, communication, transport, household, etc.; materials GaP, GaAsP - for the creation of the latest electronic technology base [1-5], as well as high-performance solar cells [6-8].

Of the mentioned types of LEDs, only GaAsP diodes doped with nitrogen can be considered highly efficient – if the maximum external quantum yield η GaP SD ≈ 1 %, then in GaAsP(N) LEDs it can reach several percent [9] further increase η^{GaP} impossible due to its indirectness. The second problem concerns both emitters – it is a significant width of the recombination volume of the diode and the adjacent base part with a high concentration of non-radiative levels. The use of direct-band materials for the formation of the active region of the LEDs and reducing its width do not contain fundamental and technological limitations and can be implemented on the basis of direct-band GaN nitride compounds, but despite their main advantage over GaP, they have the inherent disadvantages of hexagonal crystals - strong internal piezoelectric fields and spontaneous polarization (~ 10^6 V/m), which not only reduce the LEDs efficiency due to the action of the quantum-limited Stark effect, under their influence, sections of tunnel currents on the current-voltage characteristics (CVCs) [9].

The values of the ionic radii of In^{+3} cations in InN and Ga^{+3} y GaN differ by almost 1.7 times, which causes a large difference in lattice constants and, accordingly, a high density of mismatch dislocations [10, 11] when growing the InGaN active layer. Significant mechanical stresses increase the internal fields and the effect of the Stark effect, as a result, the quantum yield decreases.

The authors [12] place the main responsibility for the existence of reverse currents in InGaN diodes on helical and mixed dislocations, and it is emphasized that in III-

* Correspondence e-mail: chumak.m.e@gmail.com

Cite this article as: T.M. Zahorodnia et al., *J. Nano- Electron. Phys.* 16 No 2, 02030 (2024) https://doi.org/10.21272/jnep.16(2).02030

nitride compounds the leakage currents are significantly higher than classical diffusion or generational recombination ones. Reducing the effect of dislocations on the efficiency of the LEDs is possible by growing nanowires in the structures of the LEDs [13].

In the article [14] were discovered significant tunnel currents during direct biasing of blue InGaN LEDs.

In the InGaN LEDs, the active region is a direct-band solid solution of $In_xGa_{1-x}N$, the bandgap width of which depends on "x"; at $x = 0.2$, the diode emits blue light. An increase in the concentration of In shifts λ_{max} into the red region, at the same time, there is a drop in radiation efficiency caused by the accumulation of In atoms – an extremely negative effect, which was called the "green valley problem". The authors [10, 11] associate it with the deterioration of the crystal quality due to the mismatch of the constant lattices in InGaN and the separation of In phases, as well as with the decrease in the overlap of the electron-hole wave functions due to a strong polarization field.

The results of the study of the impact of initial structure defects and radiation-induced disturbances on GaP, GaAsP crystals and LEDs based on them are considered in the monograph [12]; The number of works devoted to the analysis of post-irradiation defects in InGaN diodes is relatively small. Given the limited scope of the article, we provide only a list of relevant references [13-24].

The quality of LEDs structures is primarily determined by the absence of failures in the operating mode, which are manifested in the form of irregularities in the CVCs or lux-ampere characteristics $L(I)$; the size of the operational resource and resistance to external factors.

To eliminate the causes and consequences of the mentioned anomalies, detailed information about the causes and sources of occurrence, formation mechanisms, reaction to the influence of external factors is necessary. The latter especially applies to the action of penetrating radiation of cosmic and terrestrial origin in conditions when these LEDs are actively used in information and communication channels of optoelectronic communication, control systems, display and processing of information flows.

The necessary results and conclusions that can contribute to the elimination of the instabilities of LEDs operation – microplasma parasitic glow, current lacing, currents flowing around; of defective tunneling or unwanted background radiation of impurities can be obtained by analyzing their electrical and spectral characteristics.

In the research materials presented below, the main focus was on the comparative analysis of CVCs of both types of LEDs with the aim of identifying the reasons that lead to deviations from the typical dependences of $I(U)$ and $L(I)$ and identifying possible physical factors that underlie the occurrence of anomalies.

2. EXPERIMENT

The original and irradiated by electrons with $E = 2$ MeV LEDs were studied: green glow grown on the basis of GaP and yellow GaAsP, as well as InGaN ($\lambda_{max} = 505$ nm, $\lambda_{max} = 470$ nm) with QW.

The dependence of the glow intensity of the green GaP LEDs on the current ($I = 2 \div 60$ mA and $I = 20 \div 60$ mA) was measured using a Green-Wave spectrometer (350-1150 nm). The CVCs of the LEDs were recorded in the range of 77÷300 K using an automatic device in the current generator and voltage generator modes.

Due to powerful air cooling during the introduction of defects, the temperature of the samples did not exceed room temperature; irradiation by electrons with $E = 2$ MeV was carried out in pulse mode.

3. RESULTS

In Fig. 1-3 show the CVCs of the original and irradiated by electrons with $E = 2$ MeV homotransient LEDs grown on the basis of GaP and GaAsP solid solution, taken in the temperature range of 77-300 K in the current generator mode.

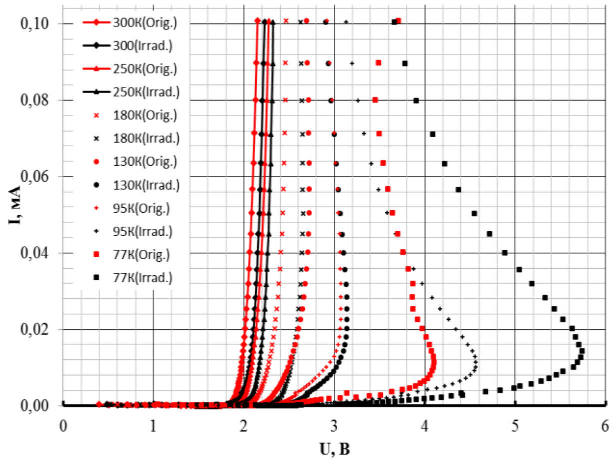

Fig. 1 – CVCs of the yellow original and irradiated ($F = 2.64 \cdot 10^{16}$ cm^{-2}, current generator mode) GaAsP LEDs, linear scale

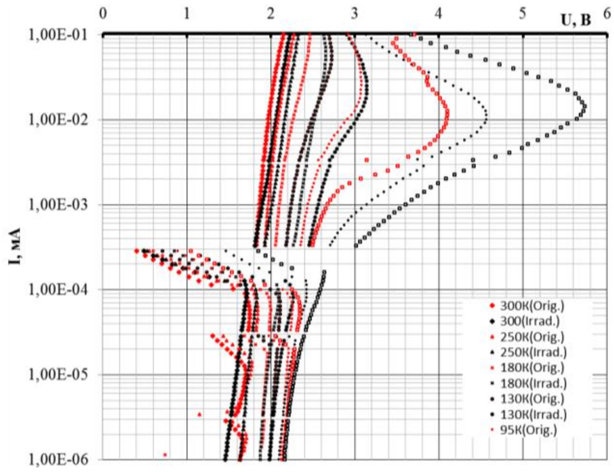

Fig. 2 – CVCs of the yellow original and irradiated ($F = 2.64 \cdot 10^{16}$ cm^{-2}, current generator mode) GaAsP LEDs, semi-logarithmic scale

It can be seen that at $T \leq 135$ K, there are areas of negative differential conductivity (NDC) on the characteristics taken in the current generator mode, which expand as the temperature decreases; at the same time, the point of transition from positive to negative resistance of the sample ("breaking point") shifts towards higher voltages (Fig. 3). At all temperatures in the range

T = 135÷77 K, the value of the positive differential resistance $(dU/dI)^+$ exceeds $(dU/dI)^-$. The introduction of radiative defects into the sample, as well as a decrease in temperature, leads to an increase in $(dU/dI)^+$ and $(dU/dI)^-$ and causes a further shift of the transition point ("breakdown point") towards higher voltages.

For example, for T = 95 = K

$$F_e = 10^{15}\text{см}^{-2}\begin{cases}\left(\frac{dU}{dI}\right)^+_{GaP,orig} \simeq 10^3\text{Ом}; & \left(\frac{dU}{dI}\right)^-_{GaP,orig} \simeq 37\ \text{Ом};\\ \left(\frac{dU}{dI}\right)^+_{GaP,irrad} \simeq 7\cdot 10^3\text{Ом}; & \left(\frac{dU}{dI}\right)^-_{GaP,irrad} \simeq 250\ \text{Ом};\end{cases} \quad 3.1$$

$$F_e = 2{,}64\cdot 10^{16}\text{см}^{-2}\begin{cases}\left(\frac{dU}{dI}\right)^+_{GaAsP,orig} \simeq 50\ \text{Ом}; & \left(\frac{dU}{dI}\right)^-_{GaAsP,orig} \simeq 2\ \text{Ом};\\ \left(\frac{dU}{dI}\right)^+_{GaAsP,irrad} \simeq 300\ \text{Ом}; & \left(\frac{dU}{dI}\right)^-_{GaAsP,irrad} \simeq 30\ \text{Ом};\end{cases} \quad 3.2$$

Therefore, when the radiation resistance of the LEDs is evaluated based on the change in the value of the diode's differential resistance $(dU/dI)^+$, it turns out that the stability of the GaAsP LEDs is significantly higher than that of the GaP LEDs (≈ 26.4 times).

The increase in (dU/dI) with decreasing temperature and with irradiation is a consequence of carrier capture by impurity levels and deep levels of radiation defects.

Extrapolation of CVCs to the zero value of I according to

$$U = I\cdot R_s + U_{p-n} \qquad (3.3)$$

makes it possible to estimate the value of the barrier potential U_{p-n}. At the doses used, the changes in the CVCs due to irradiation are due to the increase in the compensation of the electronic conductivity of the base; at the same time, the barrier potential for both types of LEDs remains practically unchanged.

In the area of small doses (up to $F = 4\cdot 10^{14}$ cm^{-2}), the current transfer mechanism of GaP LEDs remains diffusion-recombination, n- the ideality coefficient is 1.59÷1.95 (ΔT = 245÷300 K); when the temperature drops (ΔT = 135÷180 K) n = 2.64÷3.52, which indicates some growth of the tunneling component.

In GaAsP LEDs, the ideality coefficient is constant in a wider temperature range (180÷300 K), where it is equal to 2.28÷2.3; in the future, n remains unchanged up to $F = 2.64\cdot 10^{16}$ cm^{-2}. It is obvious that at such doses in the GaAsP LEDs, the concentration of introduced radiation defects is insufficient for their formation of regions of effective development of tunneling processes.

In fig. 3, 4 shows the CVCs LEDs InGaN family ($h\nu_{\max}$ = 505 nm), taken at 77÷290 K in the current generator mode, S- a similar section on the $I(U)$ curves begins to stand out upon cooling to T = 130 K. In the region of higher temperatures and significant currents, the $I(U)$ dependence becomes linear, which makes it possible to determine the series resistance of the multilayer structure of the diode Rs and the barrier potential Us. Series resistance decreases upon cooling from 10.5 Om (290 K) to 3 Om (150 K) due to its partial compensation by the negative component, which increases with decreasing temperature.

The processes that lead to the appearance of NDC in semiconductor – S diodes with current-controlled resistance are currently insufficiently investigated. It is known that current lacing in such objects can be a consequence of intervalley transfer of carriers, resonant tunneling between QWs, double injection of electrons and holes into a high-impedance depleted region, etc. [25-27].

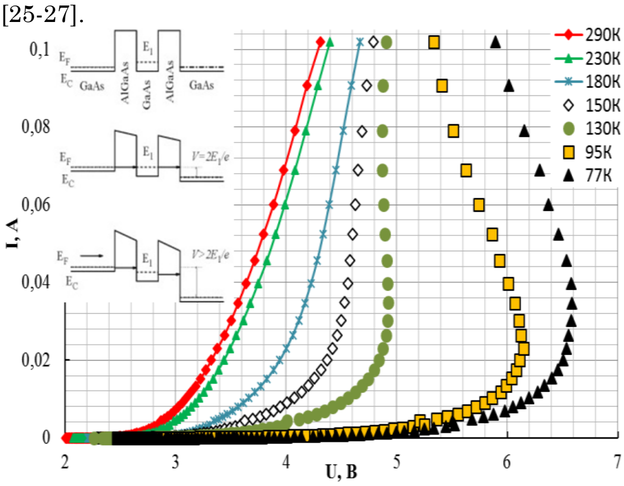

Fig. 3 – CVCs of the original green-blue ($\lambda_{\max}$ = 505 nm) InGaN LEDs are taken in current generator mode. The inset shows the diagram of inter-barrier tunneling of current carriers

One of the possible versions that can be used to explain the mechanism of NDC formation in GaP LEDs was discussed in [27], where it is emphasized that due to the peculiarities of the band structure in this crystal at low temperatures, the mechanism of intervalley scattering can be triggered.

In order to elucidate the causes of NDC in GaAsP LEDs, in which the active region is grown on the basis of a solid solution with a poorly understood band structure, additional research is needed. But, despite this, as in homojunction devices, in GaAsP LEDs, there is a high probability of the development of the process of double injection of current carriers into the depleted region of the p-n junction, which can also be implemented in the diodes we are studying.

In InGaN LEDs with QWs, much more complex than homojunctions made on the basis of GaP and GaAsP LEDs, a sharp increase in current can be caused by the resonant tunneling effect (RTE) through two barriers between adjacent QWs (Fig. 3, inset). Its high probability in InGaN LEDs is a consequence of the small thickness of barriers and pits (~ 8÷10 nm). An increase in the intensity of the electric field with a simultaneous decrease in the temperature of the sample can lead to the coincidence of the Fermi level of the left QW with the level of dimensional quantization of the right one, which manifests itself in the form of an avalanche increase in the injection of carriers.

A decrease in the barrier potential with a decrease in the diode temperature is the result of carriers moving to lower energy levels in QWs and the consequence of their capture by impurity levels in the barriers.

The values of the negative differential resistance R_S^- in the NDC section are significantly lower than R_S^+ ($R_S^- = 12{,}5$ Ом, $R_S^+ \sim 400$ Ом, 77 °K).

The mechanism of current flow at room temperature remains close to diffusion-recombination (n = 2.32); a decrease in temperature is accompanied by an increase in the contribution of the tunneling component (n= 7.5 at 77 K); already after T ≈ 230 K, the tunneling process begins to effectively affect the mechanism of current flow.

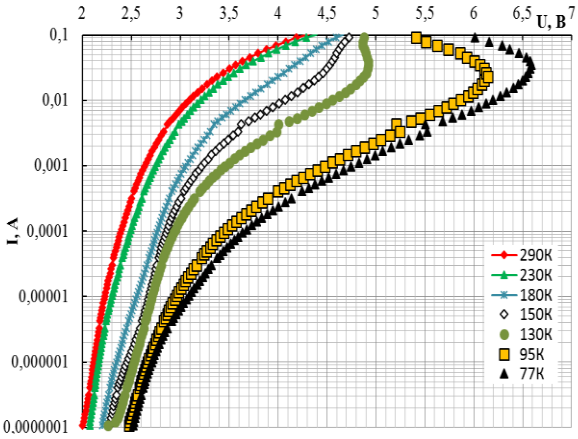

Fig. 4 – CVCs of the original green-blue (λ_{max} = 505 nm) InGaN LEDs taken in current generator mode (semi-logarithmic scale)

Within the short-wavelength halves of the emission lines ($\lambda > \lambda_{max}$) the electroluminescence spectra of GaP, GaAsP homotransient LEDs agree well with the Gaussian statistical distribution; at $\lambda > \lambda_{max}$, as can be seen from Fig. 5-6 there is a significant difference between them.

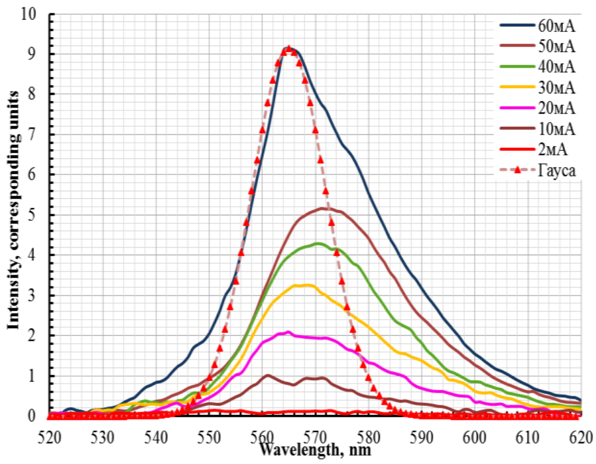

Fig. 5 – Luminance spectra of the original green GaP LED taken at different currents (I = 2÷60 mA, T = 300 K)

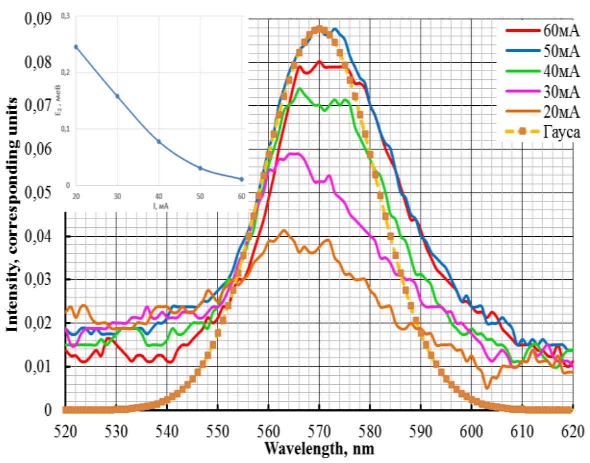

Fig. 6 – Luminescence spectra of irradiated ($F = 2\cdot10^{16}$ cm^{-2}) green GaP LEDs, taken at different currents (I = 20÷60 mA, T = 300 K). The tab shows the dependence of the Urbach energy on the current

Two mutually opposite processes – emission and absorption of light differ in general only in the direction of flow. In this case, if the Urbach energy, which characterizes the degree of crystal disorder and is determined from the slope of the near-edge absorption coefficient

$$\alpha = \alpha_0 e^{-\frac{E_g - h\nu}{E_U}} \tag{3.4}$$

then it should be equivalent to the E_2 value obtained from the slope of the long-wave wing of the spectral line of the diode emission.

On the other hand, the Urbach energy, as shown in [28], is determined by the density of charged centers N_t

$$E_U = 2{,}2W_\sigma\left(N_t - \alpha_Б^3\right)^{\frac{2}{5}}, \tag{3.5}$$

where $W_\sigma = \dfrac{e^2}{2E\alpha_Б}$; $\alpha_Б$ – the Bohr radius of matter

Therefore, it should be hoped that the observed long-wave deviation of spectral lines from the Gaussian distribution is a consequence of the effect of tails of the density of states (TDS) formed by the inhomogeneous distribution of defects in the crystal structure.

Electron irradiation leads to some increase in E_2 (E_2^{irrad}= 0.069 eV) and its small value is most likely caused by a small relative contribution of the concentration of defects of radiation origin in the presence of a high density of initial damage to the structure. After all, as it follows from the data [29], the electron dose $F = 2\cdot10^{16}$ cm^{-2} is still insufficient to achieve noticeable destruction of the absorption edge of GaP crystals.

At the same time, the decrease of the E_2 parameter with an increase in the injection current can be considered as a consequence of the "flooding" of carriers of deep levels of TDS and the glow of the participation of "Urbach tails" in the recombination process (Fig. 6, inset).

The slope of the short-wavelength wing of the spectral lines makes it possible to estimate the average temperature of the electronic subsystem. $E_1 = K_o T_e$ for I = 60 mA of the original sample is equal to $T_e \approx 441$ K in the irradiated $T_e \approx 580$ K and is practically unchanged within I = 30÷600 mA.

The growth of T_e as a result of irradiation is due to the radiation expansion of the *p-n* transition and the corresponding increase in its scattering power.

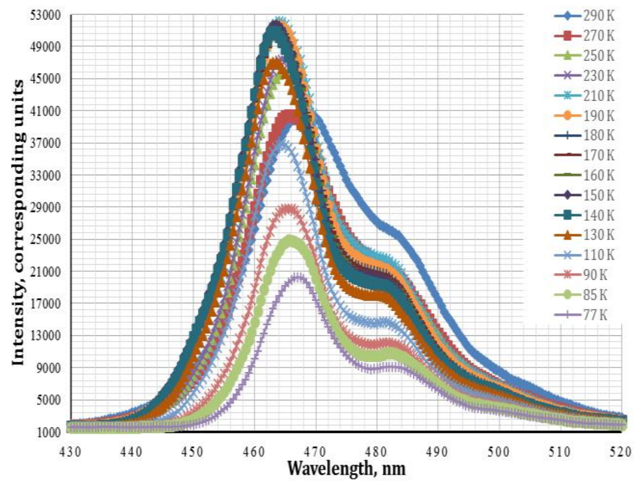

Fig. 7 – Spectral characteristics of the original InGaN LEDs (λ_{max} = 470 nm), taken at different temperatures (T = 77÷290 K, I = 16 mA)

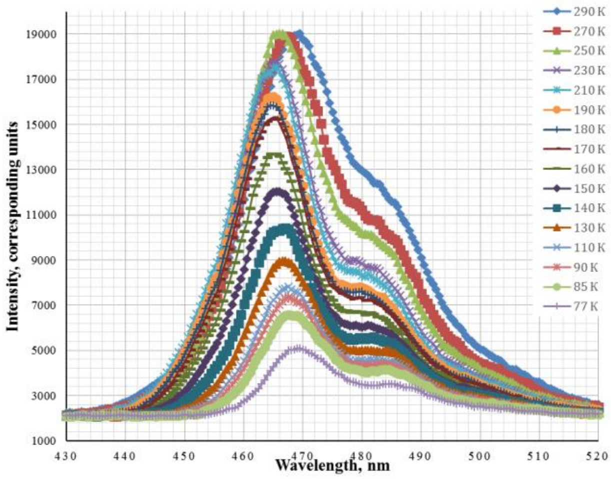

Fig. 8 – Spectral characteristics of the irradiated (F = 3.35·10^{15} cm^{-2}) InGaN LEDs (λ_{max} = 470 nm) taken at different temperatures (T = 77÷290 K, I = 16 mA)

In Fig. 7-8 show the spectra of the original and electron-irradiated InGaN heterostructure LEDs with QWs, taken in the range 77-290 K.

It can be seen that in addition to the main line of "blue" glow from λ_{max} = 465 nm, a bend is distinguished in the spectrum, the position of which is close to 480 nm, which gives reason, taking into account the data given in [30], to interpret it as a phonon repetition of the main radiation maximum.

The dependence of the intensity of the main glow of the diode on the wavelength is well approximated by the Gaussian distribution, so it is possible to estimate the line width ($\Delta\lambda$ = 14 nm), as well as the Urbach energy ($E_U = E_2^{orig}$=0.034 eV, E_2^{irrad}=0.060 eV). The temperature of current carriers in the region close to room temperature is equal to $T_e^{orig} \approx$ 375 K; $T_e^{irrad} \approx$ 479 K.

4. CONCLUSIONS

Measurements of the electrophysical characteristics of LEDs irradiated by electrons with E = 2 MeV GaP and GaAsP showed that the radiation resistance of the latter is almost 26 times higher.

The increase in the differential resistance of homotransient LEDs due to a decrease in temperature and irradiation is caused by the capture of current carriers by deep impurity levels, as well as levels of radiation defects. The value of the barrier potential of the diodes at the doses used (F_{max} = 10^{15} cm^{-2} for GaP diodes; F_{max} = 2.64 cm^{-2} for GaAsP diodes) is practically unchanged.

The current flow mechanism of GaP LEDs up to F = 4·10^{14} cm^{-2} remains diffusion-recombination (the ideality coefficient is n = 1.59÷1.95 (245÷300 K); within 135÷180 K the tunneling component increases (n = 2.64÷3.52) In GaAsP LEDs even at F = 2.64·10^{16} cm^{-2} in the interval (180÷300 K) n = 2.28÷2.3.

In InGaN heterostructure LEDs with QWs ($h\nu$ = 505 nm) the NDC region begins after cooling to $T \leq$ 130 K; its occurrence may be related to the effect of resonant tunneling of current carriers. The measured value of the series resistance of the diode, which includes the resistance of QW, barrier, buffer layers and spacer, decreases during cooling due to partial compensation by the negative component.

The current flow mechanism of the InGaN LEDs at 290 K is close to diffusion-recombination (n = 2.32); a decrease in temperature is accompanied by an increase in the contribution of the tunneling component (n = 7.5 at 77 K), which begins to effectively affect current transfer already after $T \approx$ 230 K.

The short-wavelength parts of the GaP, GaAsP, and InGaN LEDs emission lines agree well with the classical Gaussian distribution; long-wavelength ones are stretched towards long-wavelengths, which is caused by the effect of TDS in both homotransition and heterotransition structures. At the same time, the Urbach energy decreases with an increase in the injection current, which is explained by the filling of deep levels in the TDS.

It was also found that the irradiation of both types of LEDs leads to an increase in the average electronic temperature of the sample, which is associated with the radiation expansion of the p-n transition.

REFERENCES

1. *Different Types of in Light Emitting Diodes (LED) Materials and Challenges- A Brief Review BY Susan John International. Journal for Research in Applied Science & Engineering Technology (IJRASET)* **6** No IV, 4418 (2018).
2. V. Neplokh, V. Fedorov, O. Mozharov, et al., *Nanomaterials* **11** No 10, 2549 (2021).
3. *Integration of GaAsPbased III-V compound semiconductors to silicon technology* (Henri Jussila Aalto University publication series DOCTORAL DISSERTATIONS 135/2014, pp. 1-67.
4. Parsian Katal Mohseni, A.D. Rodrigues, J.C. Galzerani, Yu.A. Pusep, *J. Appl. Phys.* **106** No 12, 124306 (2009).
5. Omer Arif, Valentina Zannier, Francesca Rossi, et al. *Nanoscale* **15**, 1145 (2023).
6. Paola Prete, Daniele Calabriso, Emiliano Burresi, et al., *Materials* **16** No 12, 4254 (2023).
7. *Properties of epitaxial lateral overgrowth of GaAsP and GaAs grown by hydride vapor phase epitaxy*. (Lakshman Srinivasan Ghent University (2020).
8. Nikhil Jain, Mantu K. Hudait, *Energy Harvesting and Systems* **1** No 3-4, 121 (2014).
9. F. Shubert *LEDs*. Trans. with English under the editorship A.E. Yunovicha, 2nd ed. (M.: FIZMATLYT: 2008).
10. Y. Jiang, Y. Li, Y. Li, et al., *Sci. Rep.* **5**, 10883 (2015).
11. Anati Syahirah Hedzir, N.N. Sallehuddin, N. Saidin, Nurul Fadzlin Hasbullah, *Ukr. J. Phys. Opt.* **19** No 3, 159 (2018).
12. O.V. Konoreva, O.I. Radkevich, V.I. Slisarenko, V.P. Tartachnyk, *Effect of structural defects on the physical properties of individual semiconductor compounds* (Kyiv Academy of Sciences: Nauk. opinion, 2021).
13. Rohit Khanna, Sang Youn Han, S.J. Pearton, D. Schoenfeld, *Appl. Phys. Lett.* **87** No 21, 212107 (2005).
14. Y.L. Li, X.J. Wang, S.M. He, B. Zhang, L.X. Sun, Y.D. Li, Q. Guo, C.Q. Chen, Z.H. Chen, W. Lu, *J. Appl. Phys.* **112**, 123515 (2012).
15. S.J. Pearton et al., *ECS J. Solid State Sci. Technol.* **5**, Q35 (2016).
16. Qifeng Zhao, Xiangyang Lu, Fajun Yu, *Int. J. Opt.* **2020**, 1592695 (2020).
17. A.Y. Polyakov, et al., *J. Electrochem. Soc.* **155**, H31 (2008).
18. In-Hwan Lee, Alexander Y. Polyakov, N.B. Smirnov, *phys. status solidi (a)* **214** No 10, 1700372 (2017).
19. In-Hwan Lee, et al., *ECS J. Solid State Sci. Technol.* **6**, Q127 (2017).

20. In-Hwan Lee, A.Y. Polyakov, N.B. Smirnov, I.V. Shchemerov, P.B. Lagov, R.A. Zinov'ev, E.B. Yakimov, K.D. Shcherbachev, S.J. Pearton, *J. Appl. Phys.* **122**, 115704 (2017).
21. J.W. Tringe, A.M. Conway, T.E. Felter, W.J. Moberly Chan, et al., *IEEE Trans. Nucl. Sci.* **55** No 6, 3633 (2008).
22. Alessandro Floriduz, James D. Devine, *Jpn. J. Appl. Phys.* **57**, 080304 (2018).
23. C. Li, S. Subramanian, *IEEE Trans. Nucl. Sci.* **50** No 6, 1998 (2003).
24. Hong-Yeol Kim, Jihyun Kim, F. Ren, Soohwan Jang, *J. Vac. Sci. Technol. B* **28**, 27 (2010).
25. G. Gaydar, O. Konoreva, Ye. Maliy, Ya. Olikh, I. Petrenko, M. Pinkovska, O. Radkevych, V. Tartachnyk, *Superlattice. Microstruct.* **104**, 316 (2017).
26. E.D. Prokhorov, O.V. Botsula, *2010 International Kharkov Symposium on Physics and Engineering of Microwaves, Millimeter and Submillimeter Waves* (2010).
27. Brian R. Pamplin, *Contemporary Phys.* **11** No 1, 1 (1970).
28. V.L. Bonch-Bruevich, *UFN* **140**, 583 (1983).
29. E.Yu. Brailovsky, N.I. Ostashko, V.P. Tartachnyk, V.I. Shakhovtsov, *Ukr. Phys. J.* 26 No 6, 973 (1981).
30. V.Yu. Davydov, Yu.E. Kitaev, I.N. Goncharuk, A.N. Smirnov, J. Graul, O. Semchinova, D. Uffmann, M.B. Smirnov, A.P. Mirgorodsky, R.A. Evarestov, *Phys. Rev. B* **58**, 12899 (1998).

Властивості вихідних, опромінених електронами світлодіодних гомоперехідних GaP, GaAsP та гетероперехідних InGaN структур

Т.М. Загородня[1], О.В. Мельниченко[2], В.П. Тартачник[3], М.Є. Чумак[4]

[1] *Сумський державний університет, 40007, Суми, Україна*
[2] *Інститут фізичної хімії ім. Л.В. Писаржевського Національної академії наук України, 03028 Київ, Україна*
[3] *Інститут ядерних досліджень Національної академії наук України, 02000 Київ, Україна*
[4] *Український державний університет імені Михайла Драгоманова, 02000 Київ, Україна*

Робота містить детальний огляд опублікованих в останні роки результатів досліджень гомоперехідних світлодіодів (СД), вирощених на основі твердого розчину GaP і GaAsP, а також гетероперехідних структур InGaN з квантовими ямами (КЯ).

Для виявлення причини нестабільності світіння мікроплазми важливо проаналізувати електричні та спектральні характеристики досліджуваних структур. Метою дослідження було виявлення причини, що призводить до відхилення від типових залежностей $I(U)$ та $L(I)$ та виявлення можливих фізичних факторів, які лежать в основі виникнення аномалій світлодіодного випромінювання.

Оригінальна частина базується на порівняльному аналізі експериментальних даних, отриманих при дослідженні електрофізичних і спектральних характеристик обох типів світлодіодів.

Також наведено результати дослідження впливу радіаційних дефектів, внесених електронами з $E = 2$ МеВ, на основні та робочі параметри досліджуваних діодів.

Збільшення диференціального опору гомоперехідних світлодіодів GaP і GaAsP за рахунок зниження температури і опромінення зумовлено захопленням носіїв струму глибокими домішковими рівнями, а також рівнями радіаційних дефектів. Значення бар'єрного потенціалу діодів при використовуваних дозах ($F_{\max} = 10^{15}$ см$^{-2}$ для діодів GaP; $F_{\max} = 2{,}64$ см$^{-2}$ для діодів GaAsP) практично не змінюється.

У гетероструктурних світлодіодах InGaN з квантовими ямами ($h\nu$ = 505 нм) область НДЦ починається після охолодження до $T \leq 130$ К; його виникнення може бути пов'язане з ефектом резонансного тунелювання носіїв струму.

Короткохвильові частини ліній випромінювання світлодіодів GaP, GaAsP і InGaN добре узгоджуються з класичним розподілом Гауса; довгохвильові розтягуються в бік довгохвильових, що зумовлено ефектом хвостів густини станів як у гомо-, так і в гетеропереходних структурах.

Ключові слова: Світлодіод, GaP, GaAsP, InGaN, Вольт-амперні характеристики, Спектральні характеристики, Опромінення.